JOURNAL OF VIROLOGY, Dec. 2011, p. 13114–13123 Vol. 85, No. 24
0022-538X/11/$12.00 doi:10.1128/JVI.05759-11
Copyright © 2011, American Society for Microbiology. All Rights Reserved.

Adenovirus with Hexon Tat-Protein Transduction Domain Modification Exhibits Increased Therapeutic Effect in Experimental Neuroblastoma and Neuroendocrine Tumors▽

Di Yu,[1] Chuan Jin,[1] Justyna Leja,[1] Nadim Majdalani,[2] Berith Nilsson,[1] Fredrik Eriksson,[1] and Magnus Essand[1]*

Department of Immunology, Genetics and Pathology, Science for Life Laboratory, Uppsala University, Uppsala, Sweden,[1] and Laboratory of Molecular Biology, National Cancer Institute, Bethesda, Maryland[2]

Received 24 July 2011/Accepted 16 September 2011

Adenovirus serotype 5 (Ad5) is widely used as an oncolytic agent for cancer therapy. However, its infectivity is highly dependent on the expression level of coxsackievirus-adenovirus receptor (CAR) on the surfaces of tumor cells. Furthermore, infected cells overproduce adenovirus fiber proteins, which are released prior to cell lysis. The released fibers block CAR on noninfected neighboring cells, thereby preventing progeny virus entry. Our aim was to add a CAR-independent infection route to Ad5 to increase the infectivity of tumor cells with low CAR expression and prevent the fiber-masking problem. We constructed Ad5 viruses that encode the protein transduction domain (PTD) of the HIV-1 Tat protein (Tat-PTD) in hypervariable region 5 (HVR5) of the hexon protein. Tat-PTD functions as a cell-penetrating peptide, and Tat-PTD-modified Ad5 showed a dramatic increased transduction of CAR-negative cell lines compared to unmodified vector. Moreover, while tumor cell infectivity was severely reduced for Ad5 in the presence of fiber proteins, it was only marginally reduced for Tat-PTD-modified Ad5. Furthermore, because of the sequence alteration in the hexon HVR, coagulation factor X-mediated virus uptake was significantly reduced. Mice harboring human neuroblastoma and neuroendocrine tumors show suppressed tumor growths and prolonged survival when treated with Tat-PTD-modified oncolytic viruses. Our data suggest that modification of Ad5 with Tat-PTD in HVR5 expands its utility as an oncolytic agent.

Adenovirus serotype 5 (Ad5), which belongs to the C group of human adenoviruses, has been widely used as an oncolytic agent for cancer therapy (14, 20). Various Ad5 viruses have shown considerable therapeutic effects and have been extensively evaluated in animal models and clinical trials (7, 22, 27, 30, 44). Their advantage in cancer therapy is due to the self-propagation properties that involve replication in and lysis of infected tumor cells, which leads to secondary infection and killing of adjacent cells within the tumor. However, one limiting factor for Ad5 efficacy in cancer therapy is that the infection is dependent on coxsackievirus-adenovirus receptor (CAR) expression on target cells. CAR is an adhesion molecule expressed in tight junctions, and many cancer cells downregulate CAR expression, which results in difficulties in achieving sufficient infection and, as a consequence, the oncolytic therapeutic effect is hampered (39). One approach to circumvent this is to genetically modify Ad5 and use fibers or fiber knobs from the B group of adenoviruses, which do not bind to CAR but to other cell surface receptors (48, 49). A second limiting factor is fiber masking of receptors. This is caused by overproduction of adenovirus fiber proteins (4, 17, 31), which are released from the infected cell before cell lysis. The released fibers bind to CAR on noninfected neighboring cells, thereby limiting infection efficiency of progeny virus (31). The fiber-masking problem is not limited to the Ad5 fiber but was also observed for the Ad35 fiber, which binds to CD46 (31). These limitations must be overcome to develop successful oncolytic adenovirus agents.

Cell penetrating peptides (CPPs) have been intensively studied and widely used to deliver cargos into cells regardless of cellular specificity and independent of cell surface receptor expression. Drug delivery with CPPs has also been used in preclinical models and clinical trials (12, 35). Kurachi et al. generated a recombinant adenovirus with the protein transduction domain (PTD) of the HIV-1 Tat protein (Tat-PTD) inserted into either the HI loop or the C terminus of the viral fiber (23). Both modifications resulted in elevated transgene expression compared to unmodified virus. However, although such an oncolytic virus can overcome CAR dependency, it still uses the fiber for infection, and the excess production of fibers may block the uptake of progeny virus in neighboring cells. Eto et al. showed that adenoviruses where Tat-PTD was chemically conjugated to lysine residues on the capsid proteins, such as the adenovirus hexon, fiber, and penton base proteins, expanded the virus tropism to CAR-negative cell lines (15). Although this may be an excellent approach to expand the tropism of adenoviral vectors, it is not useful for oncolytic viruses, which rely on production of progeny virus for further rounds of infection. Only the initial virus contains the Tat-PTD modifi-

* Corresponding author. Mailing address: Department of Immunology, Genetics and Pathology, Uppsala University, SE-75185 Uppsala, Sweden. Phone: 46-18-611 0223. Fax: 46-18-611 0222. E-mail: magnus.essand@igp.uu.se.

▽ Published ahead of print on 28 September 2011.

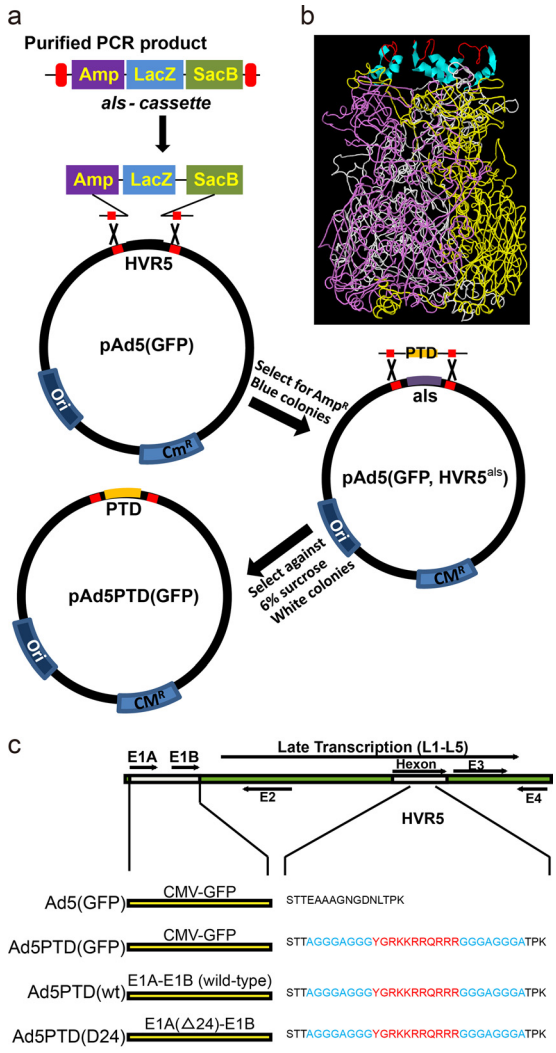

d

Viruses	evg/μL	FFU/μL	evg/FFU
Ad5(mock)	2.9×10^8	1.0×10^7	29.0
Ad5(GFP)	5.4×10^8	3.7×10^7	14.6
Ad5PTD(GFP)	1.1×10^9	9.9×10^7	11.1
Ad5(wt)	2.6×10^9	7.0×10^7	37.1
Ad5PTD(wt)	8.2×10^8	4.9×10^7	16.7
Ad5PTD(D24)	8.6×10^8	8.0×10^7	10.8

FIG. 1. Illustration of the Ad5 recombineering strategy, the predicted structure of hexon with Tat-PTD, with a schematic drawing and the titers of the viruses used. (a) An illustration of the selection-counterselection steps used for recombineering of Ad5 with the bacteriophage λ-Red system. In the first selection step, the *als* (Amp-LacZ-SacB) cassette is PCR amplified with primers that introduce 50 bp of homologous sequence to the virus genome on each side of the site of modification (in this case HVR5). The PCR product containing the *als* cassette is inserted into the modification site, and the selection is based on ampicillin resistance and blue colonies. In the second counterselection step, a PCR product is generated with the desired modification (in this case the insertion of Tat-PTD) with flanking sequences of 50 bp with homology to the virus genome on each side of the site of modification. The *als* cassette is replaced by the desired sequence, and the selection is based on sucrose and white colonies. A scarless modification has been introduced. (b) The predicted model shows the side view of a trimerized hexon with Tat-PTD in red (Trace) and α-helix spacer in cyan (Ribbon) in HVR5. The prediction was based on the online software tool (ESyPred3D Web Server 1.0), to which the amino acid sequence with the Tat-PTD modification was sent, and the original hexon structure (PDB 1P30) was selected as a template for the prediction. The software automatically gives out the prediction structure. (c) Illustration of the recombinant viruses used in the present study. (d) Titers of the viruses used in the study.

cation, and the progeny virus is not equipped to overcome CAR dependency and fiber masking.

We genetically introduced the Tat-PTD sequence on hypervariable region 5 (HVR5) of the hexon protein, the major coat protein of the virus capsid, to add a CAR-independent route of infection. We found that Tat-PTD-modified Ad5 vectors could transduce CAR-negative neuroendocrine tumor cells and that the efficacy of Tat-PTD-modified oncolytic Ad5 viruses was increased *in vitro*, which resulted in an improved therapeutic effect *in vivo*. We also found that Tat-PTD-modified oncolytic Ad5 was not blocked by soluble Ad5 fibers to the same extent as nonmodified Ad5 and that it yields larger plaques, indicating that the Tat-PTD-modified Ad5 is able to overcome the fiber-masking problem.

MATERIALS AND METHODS

Cell lines. All cell culture reagents were purchased from Invitrogen (Carlsbad, CA), except when mentioned otherwise. Cell cultures were maintained in 95% humidity incubator with a 5% CO_2 atmosphere at 37°C. The cell lines BON (kindly provided by J. C. Thompson and C. M. Townsend, Galveston, TX), CNDT2.5 (13, 43) (kindly provided by L. M. Ellis, M.D. Anderson, Houston, TX), SKOV-3 (American Type Culture Collection [ATCC], Manassas, VA), A549 (ATCC), MB49, 911 (Crucell, Leiden, Netherlands), 1064SK, and mel526 (kindly provided by T. Boon, LICR, Brussels, Belgium) were cultured as described elsewhere (28). The human neuroblastoma cell line SK-N-SH (kindly provided by F. Hedborg, Uppsala University, Uppsala, Sweden) was cultured in minimal essential medium supplemented with 10% fetal bovine serum (FBS), 1 mM NaPyr, and PEST. The human umbilical vein endothelial cell line HuVec (3H Biosciences, Uppsala, Sweden) was cultured in endothelial cell growth medium MV2 supplemented with 5 ng of hEGF/ml, 0.5 ng of hVEGF/ml, 20 ng of R3 IGF/ml, 200 ng of hydrocortisone/ml, 10 ng of hbFGF/ml, and 1 μg of ascorbic acid (PromCell, Heidelberg, Germany)/ml. The Rmcb hybridoma cell line, which secrete anti-CAR antibodies, was purchased from the ATCC and maintained in RPMI 1640 supplemented with 10% FBS.

Flow cytometry. The CAR expression level on the cell lines were assessed by flow cytometry as described elsewhere (28).

Recombinant adenoviruses construction by λ-Red recombineering. All recombinant adenovirus outlined in Fig. 1a were generated based on λ-phage mediated-recombineering in *Escherichia coli* strain SW102 using bacmid pAdZ5-CV5-E3+ (kindly provided by Richard Stanton, Cardiff University, Cardiff, United Kingdom) (38). This bacmid contains the Ad5 genome, with the E1 region replaced by a selection/counterselection cassette (*als* cassette) consisting of the *bla* (ampicillin resistance), *lacZ* (β-galactosidase), and *sac*B (sucrose resistance) genes. To generate pAd5(GFP), the cytomegalovirus promoter-green fluorescent protein (CMV-GFP) cassette was PCR amplified from Ad5(GFP) (28) using the primers pF.Shuni and pR.Shuni and purified by gel extraction. Heat-activated and freshly made competent *E. coli* SW102 cells containing pAdZ5-CV5-E3+ were electroporated with 100 ng of PCR product by using the Gene Pulser II (Bio-Rad Laboratories, Hercules, CA). Selection was performed on LB-sucrose plates, containing LB without NaCl, 6% sucrose, 200 μM IPTG (isopropyl-β-D-thiogalactopyranoside; Sigma-Aldrich, St. Louis, MO), and 40 μg of X-Gal (5-bromo-4-chloro-3-indolyl-β-D-galactopyranoside; Invitrogen)/ml. Positive colonies were designated pAd5(GFP).

To generate a scar-free modification in hexon HVR5, a selection-counterselection method was used. The general procedure is described in Fig. 1a. Briefly, the *als* cassette was PCR amplified using the primers pF.HVR5-als and pR.HVR5-als and knocked into the HVR5 site in pAd5(GFP). Selection was performed on LB agar plates containing 100 μg of ampicillin/ml, 200 μM IPTG, and 40 μg of X-Gal/ml. Positive colonies were designated pAd5(GFP, $HVR5^{als}$). Next, the *als* cassette was replaced by the Tat-PTD motif to generate

TABLE 1. Primers used in this study

Primer	Sequence (5′–3′)[a]
pF.Shuni	GATTTGGCCATTTTCGCGGG
pR.Shuni	GGCGGCTGCTGCAAAACAGAT
pF.HVR5-als	AATGGAAAGCTAGAAAGTCAAGTGGAAATGCAATTTTTCCCTGTGACGGAAGATCACTTCG
pR.HVR5-als	CCACTTTAGGAGTCAAGTTATCACCATTGCCTGCGGCTGCCTGAGGTTCTTATGGCTCTTG
pF.E1-als	CTGAATAAGAGGAAGTGAAATCTGAATAATTTTGTGTTACTCATAGCGCG*GGATCC*CCTGTGACGGAAGATC
pR.E1-als	GATACAAAACTACATAAGACCCCCACCTTATATATTCTTTCCCACCC*GGATCC*CTGAGGTTCTTATGGC
pF1.HVR5-PTD	CCCCAATGAAACCATGTTAC
pR1.HVR5-PTD	**TCTTCGTCGCTGTCTCCGCTTCTTCCTGCCATATCCACCTCCAGCTCCACCTCCAGC**AGTAGTTGAGAAAAATTGCA
pF2.HVR5-PTD	**TATGGCAGGAAGAAGCGGAGACAGCGACGAAGAGGAGGTGGAGCTGGAGGTGGAGCT**ACTCCTAAAGTGGTATTGTAC
pR2.HVR5-PTD	GCAATGTAATTAGGCCTGTTG
Ad.Titration.F	CATCAGGTTGATTCACATCGG
Ad.Titration.R	GAAGCGCTGTATGTTGTTCTG

[a] Sequences with homologous regions are underlined. PTD modification sequences are indicated in boldface. Restriction sites are indicated in italics.

pAd5PTD(GFP). Selection was performed on LB-sucrose plates. The Tat-PTD motif fragment was generated by joint PCR with the primer pairs pF1.HVR5-PTD/pR1.HVR5-PTD and pF2.HVR5-PTD/pR2.HVR5-PTD.

pAd5PTD(wt) and pAd5PTD(D24) were generated in the same manner by replacing the CMV-GFP cassette from the E1 region with serotype 5 wild-type E1A-E1B or E1A(D24)-E1B sequences. The *als* cassette was amplified by using the primers pF.E1-als/pR.E1-als to replace the CMV-GFP cassette. pF.Shuni and pR.Shuni were used for amplification of either the E1 region from wild-type adenovirus DNA or the E1-D24 region from plasmid AdEasy(D24).fk3 (kindly provided by A. Hemminki, Helsinki University, Helsinki, Finland). The PCR products were then used for replacement of the *als* cassette in the E1 region to generate pAd5PTD(wt) and pAd5PTD(D24), respectively. The viruses generated from pAd5PTD(GFP), pAd5PTD(wt), and pAd5PTD(D24) were named Ad5PTD(GFP), Ad5PTD(wt), and Ad5PTD(D24). A predicted (24) model of the trimerized hexon with Tat-PTD in HVR5 based on published hexon structure (33) (PDB 1P30) is presented in Fig. 1b. All viruses used in the present study are described in Fig. 1c. All primers used can be found in Table 1.

Virus production and titration. Wild-type Ad5 (ATCC) was propagated in A549 cells, while all other genetically modified viruses were propagated in 911 cells (16). The replication-defective E1/E3-deleted AdMock, referred to here as Ad5(mock), was described earlier (6). All viruses were purified by CsCl gradient ultracentrifugation, dialyzed against a viral storage buffer (10 mM Tris-HCl [pH 8.0], 2 mM $MgCl_2$, 4% [wt/vol] sucrose) as described previously (7, 26), and stored in aliquots at −80°C.

Since the viral surface protein was modified in the present study, the infectious virus titer will depend on cell line used for titration. Therefore, virus titers (encapsidated viral genomes) were determined by real-time quantitative-PCR (40). Briefly, viral DNA was extracted by using a High Pure viral nuclear acid kit (Roche, Mannheim, Germany). The DNA copy number was detected by using the primers Ad.Titration.F and Ad.Titration.R targeting the adenovirus E4 ORF1 region. Plasmid, pCR2.1(AdE4orf1), containing the same amplicon, was used for the generation of standard curve (10). Virus titer was calculated as the mean of three independent experiments. The titer was designated as encapsidated viral genome(s) (evg). A fluorescent forming unit (FFU) assay on 911 cells was also used to determine the infectious virus titers (9). The evg/μl, FFU/μl, and evg/FFU ratios of the viruses used in the present study are given in Fig. 1d. We used fixed evg when comparing the viruses on the various cell lines.

Transduction efficiency assay. Cells were de-attached and mixed with appropriate amount of GFP-containing virus at different evg/cell at 37°C for 2 h in a volume of 200 μl. Free virus was washed away after transduction, and cells were seeded in 24-well plates. The percent GFP-expressing cells was evaluated by flow cytometry (FACSCalibur; BD Biosciences, Franklin Lakes, NJ) after 48 h.

Cell viability assay. Cells were transduced with virus in suspension for 2 h with different evg per cell and then seeded in a 96-well plate in a total volume of 100 μl (1,000 cells/well for SK-N-SH and 5,000 cells/well for CNDT2.5). Cell viability was evaluated at day 4 by using a MTS Cell Titer Aqueous One Solution cell proliferation assay kit (Promega, Madison, WI). The relative cell viability was calculated by using the ratio between the average absorbance for viral transduced cells and the average for nontransduced cells.

***In vitro* viral replication assay.** Cells were seeded in 24-well plates to 80% confluence and transduced with virus at 500 evg/cell. The transduction medium was replaced by cell culture medium after 2 h. Viral genomic DNA was isolated directly after transduction (day 0) and at days 1, 2, and 3 and then quantified by real-time PCR. Relative viral replication was presented as the fold increase in genomic DNA copy number.

Western blotting. SK-N-SH cells were transduced in suspension with Ad5PTD(GFP), Ad5(wt), Ad5PTD(wt), and Ad5PTD(D24) at 500 evg/cell and cultured in 12-well plates. Cells were harvested 48 h later, and total protein extracts were prepared. E1A and β-actin protein expression was detected as described previously (26), with minor modifications. In brief, the membrane was incubated with a mouse monoclonal anti-E1A antibody (M73; Neomarkers, Inc., Fremont, CA) and a goat polyclonal anti-β-actin antibody (Santa Cruz Biotechnology, Santa Cruz, CA). After a washing step, the membrane was incubated with rabbit anti-mouse 680 antibody (Invitrogen) and donkey anti-goat 800 antibody (Odyssey Infrared Imaging/LI-COR Biosciences, Lincoln, NE). The membrane was then scanned using the Odyssey infrared imaging system (LI-COR Biosciences).

Fiber blocking assay. Soluble Ad5 fiber molecule was obtained as described previously (31). A549 cells were transduced at 500 evg/cell with Ad5(GFP) or Ad5PTD(GFP) in the presence or absence of fiber molecules (500 μl) for 2 h. The cells were then washed once and seeded in a 24-well plate. After 48 h, GFP-expressing cells were analyzed by flow cytometry.

Plaque formation assay. A standard plaque formation assay with neutral red staining as described previously (42) was performed to visualize plaques. In brief, monolayer A549 cells in a six-well plate were transduced with 100 evg of either Ad5(wt) or Ad5PTD(wt). The medium was removed, and the cells were washed once with phosphate-buffered saline (PBS) and overlaid with low-melting-point agar. After 5 days the cells were once more overlaid with low-melting-point agar containing neutral red (Sigma) for visualization of plaques, and the plates were thereafter inspected daily. Plaques were measured on day 8 after viral transduction by using an eyepiece graticule and visualized by scanning the plate.

FX-mediated adenovirus binding assay. SKOV3 cells were plated in a 24-well plate at 10^5 cells/well. The next day, the cells were incubated with virus in the presence or absence of the physiological level of coagulation factor X (FX; 8 μg/ml) (Hematologic Technologies, Inc., Essex Junction, VT) at 500 evg/cell in a total volume of 300 μl at 4°C for 1 h while rocking. Thereafter, the supernatant was replaced by cell culture medium. Viral genomic DNA was isolated directly after incubation using a High Pure viral nucleic acid kit (Roche) and quantified by real-time PCR as described above for virus titration.

Either Ad5(wt) or Ad5PTD(wt) were mixed with reactive fluorescein isothiocyanate (FITC) at a ratio of 1 μg of FITC per 10^{10} evg viruses in borate buffer (pH 9.0), followed by incubation for 1 h at 37°C. The FITC-labeled viruses were then dialyzed against PBS. Real-time measurements of the binding of FITC-labeled viruses to SKOV3 cells was performed at room temperature in LigandTracer Green (Ridgeview Instruments AB, Uppsala, Sweden), essentially according to a previously published protocol (3). Compared to surface plasma resonance, LigandTracer Green is an alternative instrument for monitor virus-cell interaction. Briefly, a baseline was generated by incubation of cells in 3 ml of culture medium. The cells were then incubated for ~2 h with 5,000 evg FITC-labeled viruses in the presence or absence of FX (8 μg/ml), while the association rates were recorded. After incubation, the virus solution was replaced with fresh medium, and the dissociation rate was monitored and recorded.

Neutralization assay. Neutralizing antibody (NAb) was prepared by immunizing mice with adenovirus followed by isolation of plasma from whole blood. Briefly, BALB/c mice were injected intraperitoneally with Ad5(mock) at 10^{10} evg/mouse and boosted twice with the same amount of virus with 2-week intervals. Plasma was isolated from whole blood by centrifugation at 3,000 × *g* for 20 min at 4°C. The plasma was heat inactivated at 56°C for 1 h. Ad5(GFP) and Ad5PTD(GFP) were then mixed with plasma dilutions (1:10 to 1:1,000,000) in a 96-well plate at 10^6 evg with a volume of 100 μl/well. The plate was incubated at

37°C for 1 h. Subsequently, 10^5 911 cells were added in a volume of 100 μl to each well. After 24 h of incubation, the cells were analyzed for GFP expression by flow cytometry (BD LSR II flow cytometer; BD sciences).

Animal studies and tumor models. Female, SCID/beige mice (3 to 4 weeks old) were purchased from Taconic (Denmark). Male, NMRI-nude mice (3 to 4 weeks old) were purchased from Harlan (Germany). All mice were housed at the Rudbeck animal facility (Uppsala, Sweden) in individually ventilated cages (three mice per cage). Tumor implantation was performed 1 week after mouse delivery.

Neuroblastoma cells (10^6 SK-N-SH) were mixed 1:1 (vol/vol) with Matrigel (BD Biosciences) in a total volume of 50 μl and injected subcutaneously into the hind flank of SCID/beige mice. Mice were treated with peritumoral injections of either Ad5(wt), Ad5PTD(wt), Ad5PTD(D24), or PBS on days 10, 12, 14, and 16 at a dose of 5×10^9 evg/injection in 30 μl. Six mice per group were used. Tumor growth was monitored by caliper measurement. Tumor size was calculated using an ellipsoid volume formula (length × width × depth × π/6). The experiment was terminated directly after the last mouse was sacrificed in the Ad5(wt)-treatment group.

Neuroendocrine tumor cells (5×10^6 CNDT2.5) were mixed 1:1 (vol/vol) with Matrigel in a total volume of 100 μl and injected subcutaneously in the hind flank of NMRI-nude mice. Mice were treated with intratumoral injections of either Ad5(mock), Ad5PTD(D24), or PBS on days 17, 19, 21, and 23 at a dose of 5×10^9 evg/injection in 30 μl. Six mice per group were used. Tumor growth was monitored by caliper measurement. Tumor size was calculated using an ellipsoid volume formula (length × width × depth × π/6).

Statistical analysis. Statistical analysis was performed by using GraphPad Prism software version 5.01 (GraphPad Software, San Diego, CA). An unpaired Student *t* test was used to compare the transduction efficiency, MTS cell killing assay, viral replication assay, fiber blocking assay, anti-CAR antibody blocking assay, and neutralization assay. A Mann-Whitney test was performed to compare plaque sizes in plaque formation assay. Log-rank test was used to compare survival curves created by the Kaplan-Meier method. Tumor sizes in different treatment groups were compared by using two-way analysis of variance.

Biosafety level and ethics declaration. The Swedish Work Environment Authority approved the work with genetic modification of the infectious capacity of human adenovirus serotype 5 (ID number 202100-2932 v66a13 [laboratory] and v66a9 [mice]) and genetic modification of replication capacity of human adenovirus serotype 5 (ID number 202100-2932 v66a11 [laboratory] and v66a7 [mice]). All experiments regarding modified adenoviruses were conducted under biosafety level 2. The Uppsala Animal Ethics Committee approved the animal studies (ID number C319/9).

RESULTS

A Tat-PTD-modified adenoviral vector can efficiently transduce CAR-negative cells. Adenoviral vectors are widely used as gene transfer vehicles. They efficiently introduce foreign genes into cells expressing CAR, the native receptor for Ad5 infection. We compared the gene transduction capacity of two GFP-expressing adenoviral vectors in a range of cell lines. Ad5(GFP) uses the same infection route as wild-type Ad5, while Ad5PTD(GFP), in addition to the Ad5 infection route, has the Tat-PTD sequence in HVR5 of the hexon protein on the virus capsid. SK-N-SH, MB49, CNDT2.5, and 1064SK are CAR negative or have low CAR expression levels, whereas A549, mel526, HuVec, and BON express moderate to high levels of CAR (Fig. 2). Ad5PTD(GFP) showed efficient transduction of CAR-negative cell lines, whereas Ad5(GFP) showed no or very poor transduction of these cells (Fig. 2). Furthermore, transduction of CAR-positive cell lines by Ad5PTD(GFP) was always more efficient or as efficient as transduction with the unmodified Ad5(GFP) (Fig. 2). These results indicate that insertion of a small cell penetrating peptide into the adenoviral hexon protein surface HVR5 region dramatically enhances adenovirus transduction ability.

Tat-PTD-modified oncolytic adenoviruses yield enhanced cell killing. Genetically engineered oncolytic adenoviruses have been tested in several clinical cancer trials. Therefore, we wanted to investigate whether the oncolytic ability of Ad5 could be enhanced by the Tat-PTD modification. Two replication-competent Tat-PTD-modified adenoviruses were produced. Ad5PTD(wt) is a wild-type adenovirus with Tat-PTD in HVR5, and Ad5PTD(D24) is a Tat-PTD-modified virus with a 24-bp deletion in E1A, which confers selectivity to replication in pRb pathway-deficient cancer cells (2, 19). *In vitro* cell killing and viral replication assays were performed. The Ad5PTD(wt) and Ad5PTD(D24) viruses exhibited significantly ($P < 0.001$ at 1,000 evg/cell) increased the killing ability of CAR-negative neuroblastoma and neuroendocrine tumor cells compared to unmodified wild-type virus Ad5(wt) (Fig. 3a). Furthermore, Ad5PTD(wt) and Ad5PTD(D24) yielded significantly ($P < 0.001$ at day 3) higher numbers of progeny virus compared to Ad5(wt) (Fig. 3b). The increased cell killing

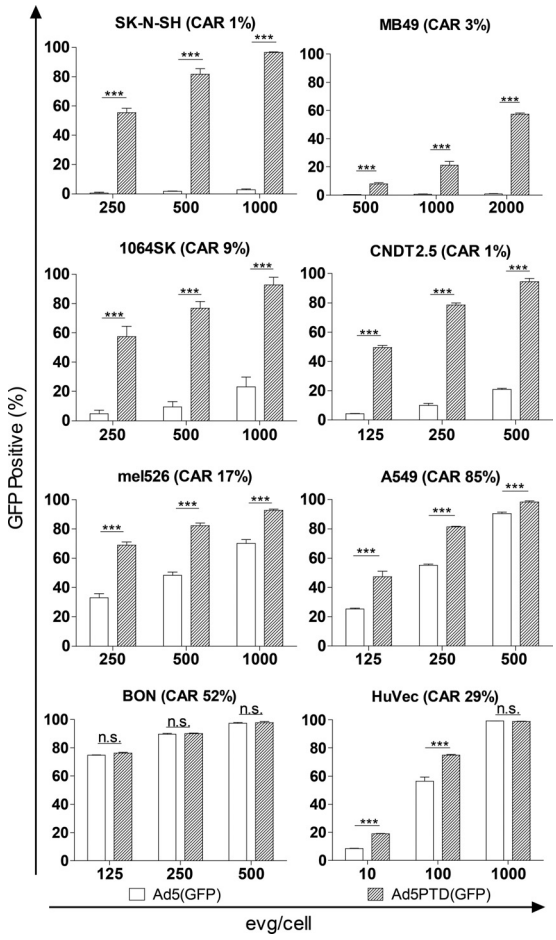

FIG. 2. A Tat-PTD-modified Ad5 vector can transduce cells with low CAR expression. Cells were transduced in suspension for 2 h with GFP-expressing adenoviral vectors at various levels of evg/cell. The viral vector was then washed away, and the cells were analyzed by flow cytometry 48 h after transduction. Values are shown as means + the standard deviation (SD) from three independent experiments, each with triplicate samples. An unpaired Student *t* test was used for comparison (***, $P < 0.001$; not significant [n.s.], $P > 0.05$; $n = 3$). The values in parenthesis after each cell line name indicate the CAR expression level (percentage of CAR-positive cells), as assessed by fluorescence-activated cell sorting staining.

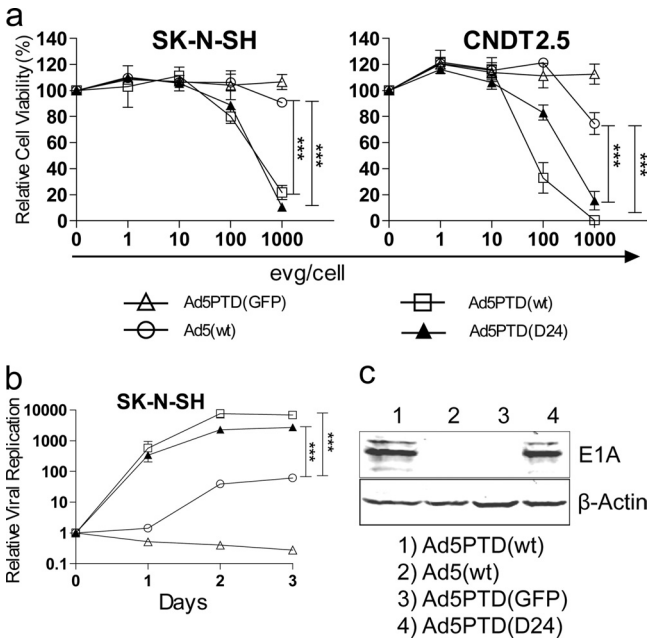

FIG. 3. Tat-PTD-modified oncolytic adenoviruses yield enhanced cell killing and replication activities. (a) A neuroblastoma (SK-N-SH) and a neuroendocrine tumor (CNDT2.5) cell lines, both with low CAR expression, were transduced with Tat-PTD-modified or wild-type Ad5 virus at various levels of evg/cell. The non-replication-competent Tat-PTD-modified viral vector Ad5PTD(GFP) was used as a negative control. The relative cell viability was analyzed 4 days after transduction by MTS assay. The data are shown as means ± the SD from three independent experiments, each with triplicate samples (***, $P < 0.001$; $n = 3$). (b) Neuroblastoma (SK-N-SH) cells were transduced with virus at 500 evg/cell. Viral genomic DNA was isolated at days 0, 1, 2, and 3 after transduction and quantified by using real-time PCR. Values show the fold change in relation to day 0 (set to 1). The data are shown as means ± the SD from three independent experiments, each with triplicate samples (***, $P < 0.001$; $n = 3$). (c) SK-N-SH cells were transduced with virus at 500 evg/cell. Total protein lysates were prepared after 48 h, and 50-μg samples were resolved by SDS-PAGE. E1A was detected by Western blotting with an anti-E1A antibody. β-Actin was used as a loading control.

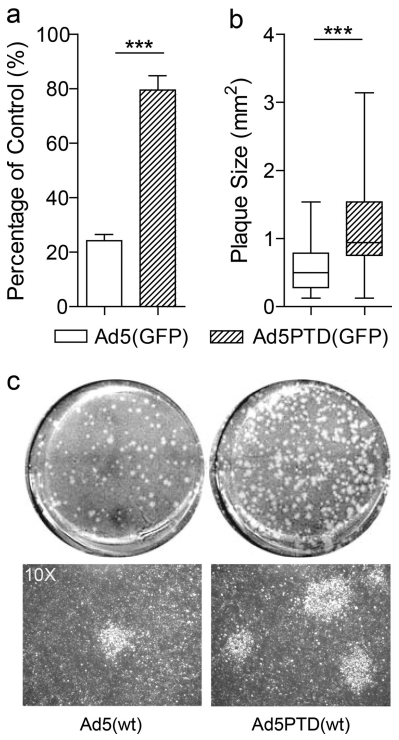

FIG. 4. A Tat-PTD-modified oncolytic adenovirus overcomes the fiber-masking problem and spreads more efficiently than a nonmodified virus. (a) A549 cells were transduced with GFP-expressing adenoviral vectors at 500 evg/cell in the presence of free soluble Ad5 fiber molecules and analyzed by flow cytometry after 2 days. Transduced cells in the absence of soluble Ad5 fiber served as control (set to 100%) (***, $P < 0.001$; $n = 3$). (b) Monolayer A549 cells were transduced with equal amount of either Ad5(wt) or Ad5PTD(wt), followed by a low-melting-point agar overlay and neutral red staining. Plaque sizes measured after 8 days are represented as whisker box plot with median, lower quartile, upper quartile, minimum, and maximum values. A comparison was performed by the nonparametric Mann-Whitney test (***, $P < 0.001$, $n = 50$). (c) Representative images of the whole well from the plaque formation assay at day 8, formed by Ad5(wt) and Ad5PTD(wt). Corresponding pictures (×10 magnification) are shown as well.

and replication are tributes to higher transduction efficacy. Interestingly, Ad5(wt) did replicate in SK-N-SH cells to a certain degree but did not exhibit any killing ability in this cell line, not even at 1,000 evg/cell, most likely due to the inability to achieve a high enough transduction level of these cells (Fig. 3a and b), while the Tat-PTD-modified viruses showed both killing and replicating activities (Fig. 3a and b). Western blot analysis detects E1A protein expression in SK-N-SH cells only after transduction with the Tat-PTD-modified viruses, indicating once more that the transduction rate of wild-type Ad5 is very low in this cell line (Fig. 3c). These results show that the Tat-PTD modification can broaden the viral transduction ability with gain in killing of CAR-negative cells and without any loss of oncolytic capacity in CAR-positive cells (data not shown).

Tat-PTD-modified adenovirus overcomes the fiber-masking problem, leading to an increase in oncolytic virus spread. The adenovirus fiber protein is expressed in huge excess during the cycle of viral infection and replication (4, 17, 31). Recently, it was reported that the excess fiber proteins, which are released to the environment before mature viral particles lyse the infected cells, masks the receptors on uninfected cells in the vicinity, thereby preventing the second round of progeny virus infection (31). This property hampers the spread of oncolytic virus within tumors. Since the Tat-PTD-modified virus has a CAR-independent entry mechanism, we compared gene transfer activity of Ad5(GFP) and Ad5PTD(GFP) in the presence of excessive soluble fiber molecules. GFP expression in cells transduced with Ad5(GFP) in the presence of soluble fiber was reduced to 20% compared to that in the absence of soluble fiber. However, cells transduced with Ad5PTD(GFP) retained 80% transduction efficacy in the presence of soluble fiber (Fig. 4a). Furthermore, we performed a plaque formation assay to evaluate virus spread during replication. The plaques formed by Ad5PTD(wt) started to be visible at day 3, while the plaques formed by Ad5(wt) started to be visible at day 6. At day 8, the plaques formed by Ad5PTD(wt) were on average 1.6 times larger than the plaques formed by Ad5(wt) (Fig. 4b). A representative data set of the plaques formed by both viruses is

shown in Fig. 4c, with entire wells shown in the upper panel and photographs with ×10 magnification pictures of the plaques shown in the lower panel. These results indicate that viruses with the Tat-PTD-modification can overcome the fiber-masking problem and thus enhance the second round of infection by progeny virus. Moreover, these results further strengthen the notion that the Tat-PTD-modified virus can enter the cells via a CAR-independent pathway.

Tat-PTD-modified Ad5 vector can resist FX-mediated uptake and partially overcome anti-Ad5 antibody neutralization. It has been reported that viral transduction of hepatocytes is mediated by binding of coagulation factor X (FX) to the hypervariable region of the Ad5 hexon surface (47). We investigated whether our Tat-PTD modification could reduce the FX-mediated viral uptake by incubating SKOV3, a cell line commonly used to demonstrate FX-mediated Ad5 uptake, with or without physiological concentrations of FX. By real-time measurements of virus-cell interactions using LigandTracer Green, we found that FITC-labeled Ad5PTD(wt) showed far less FX-mediated binding to SKOV3 cells than FITC-labeled Ad5(wt) during the retention phase (Fig. 5a). These results were confirmed by real-time quantitative PCR measurement of viral genome copies associated with the cells after binding. For the real-time PCR experiments, the viral binding ability of the unmodified Ad5(GFP) vector was ca. 20 times higher than the binding of the Tat-PTD-modified Ad5PTD(GFP) vector to the cell surface of SKOV-3 cells in the presence of FX (Fig. 5b). Taken together, these results indicate that the small modification of introducing Tat-PTD in HVR5 significantly altered FX-mediated viral uptake.

One limitation of using oncolytic adenovirus for cancer virotherapy is the high prevalence of neutralizing anti-Ad5 antibodies (32), which may limit the use of intravenous administration of Ad5. We investigated whether the Tat-PTD modification conferred the ability to escape from existing NAbs. Mice were immunized with unmodified Ad5. Plasma was isolated from the immunized mice and used to perform *in vitro* neutralization assay. Tat-PTD-modified viruses were moderately protected from NAbs. There was a trend toward protection for all plasma dilution points, but only two points reached statistically significant differences (Fig. 5c).

Treatment with Tat-PTD-modified oncolytic adenoviruses delays tumor growth and prolongs survival in mice carrying xenografted human neuroblastoma and neuroendocrine tumors. To evaluate the oncolytic viruses as therapeutic agents *in vivo*, SCID/beige mice harboring human neuroblastoma (SK-N-SH) and NMRI-nude mice harboring human neuroendocrine tumors (CNDT2.5) were used. Tumor cells were implanted subcutaneously on the right hind flank. Once established, SK-N-SH tumors on SCID/beige mice were treated with peritumoral injections of Tat-PTD-modified viruses or Ad5(wt), while PBS was used as a control. CNDT2.5 tumors on NMRI-nude mice were treated with intratumoral injections of Ad5PTD(D24), while Ad5(mock) and PBS were used as controls. Tumor growth was monitored by caliper measurements.

In the SK-N-SH xenograft model, mice treated with either Ad5PTD(wt) or Ad5PTD(D24) showed a significant ($P < 0.001$) suppression of tumor growth (Fig. 6a) and prolonged survival compared to mice treated with Ad5(wt) (Fig. 6b).

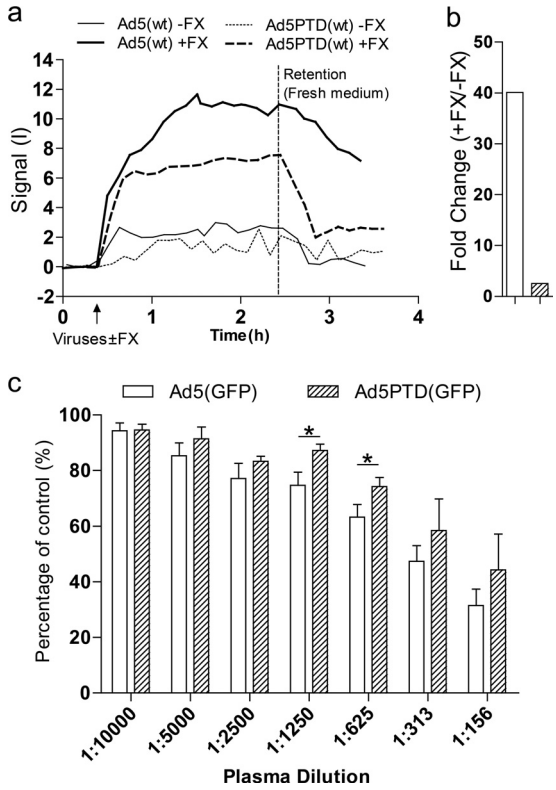

FIG. 5. Tat-PTD-modified Ad5 vector can resist FX-mediated uptake and partially overcome anti-Ad5 antibodies. (a) A total of 5,000 evg of either FITC-labeled Ad5(wt) or FITC-labeled Ad5PTD(wt) in 3 ml of culture medium was added to monolayer SKOV3 cells, covering a small portion of the culture dish, in the presence or absence of FX (8 μg/ml). The FX-mediated virus-cell binding interaction was measured and recorded in real-time by using LigandTracer Green. Representative data from one experiment out of three are shown. (b) Monolayer SKOV3 cells were transduced for 1 h at 4°C with GFP-expressing adenoviral vectors at 500 evg/cell in the presence of FX (8 μg/ml). Transduced cells without the addition of FX served as a control (set to 100%). Viral genomic DNA was isolated directly after transduction and quantified by real-time PCR. Representative data from one experiment out of two are shown. (c) A549 cells were transduced with GFP-expressing adenoviral vectors at 500 evg/cell in the presence of heat-inactivated mouse plasma, from mice immunized with Ad5(mock), at various dilutions and analyzed by flow cytometry after 24 h. Transduced cells in the absence of mouse serum served as control (set to 100%). The data are presented as means + the SD from at least three independent experiments, each with triplicate samples. A Student *t* test was performed to evaluate statistical differences (***, $P < 0.001$; *, $P < 0.05$; n.s., $P > 0.05$).

Interestingly, there was no difference between Ad5(wt)-treated mice and PBS-treated mice, reflecting the lack of Ad5(wt) transduction of SK-N-SH cells.

In the CNDT2.5 xenograft model, mice treated with Ad5PTD(D24) showed a significant ($P < 0.001$) suppression of tumor growth compared to mice treated with the replication-defective virus Ad5(mock) or PBS (Fig. 6c). Although there was a significant tumor growth suppression for Ad5(mock)-treated mice compared to PBS-treated mice, no mice were cured in the Ad5(mock) treatment group. Moreover, mice treated with Ad5PTD(D24) showed a significantly prolonged survival compared to PBS-treated mice and Ad5(mock)-

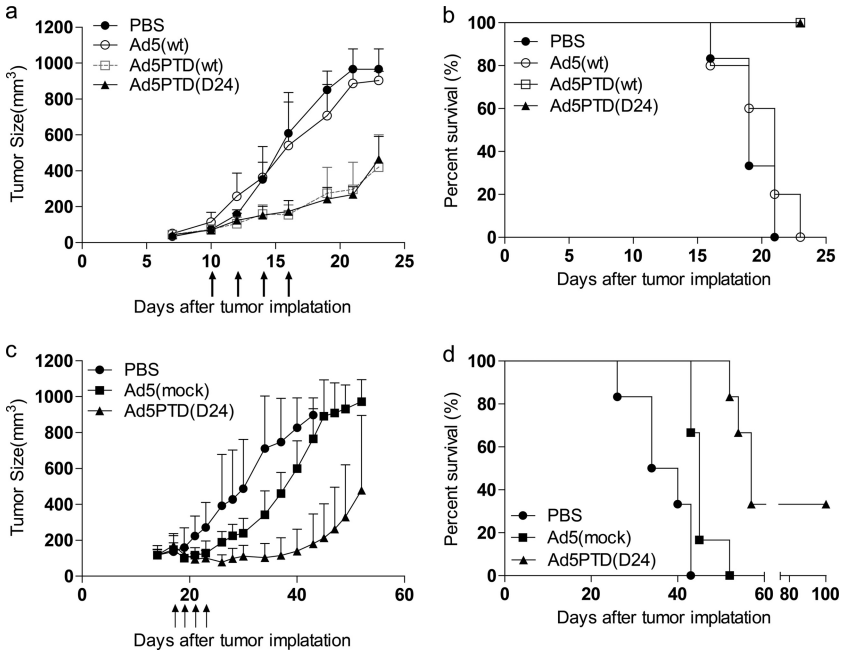

FIG. 6. Treatment with Tat-PTD-modified oncolytic adenoviruses delay tumor growth and prolong survival in mice with transplanted human neuroblastoma and neuroendocrine tumors. (a) SCID/beige mice harboring subcutaneous neuroblastoma, SK-N-SH, were treated by peritumoral virus injections, as indicated by the arrows. (c) NMRI-nude mice harboring subcutaneous neuroendocrine tumor, CNDT2.5, were treated by intratumoral virus injections as indicated by arrows. The tumor volume was monitored by caliper measurements. Six mice per group were used, and the data represent means + the SD. Mice were sacrificed when the tumor size reached 800 mm^3. The experiment of SCID/beige mice was terminated when the last mouse in the Ad5(wt) treatment group was sacrificed due to wounds on the tumors. The experiment with NMRI-nude mice was terminated at day 100 after tumor implantation. A Kaplan-Meier survival curve shows the survival data (b, SCID/beige mice; d, NMRI-nude mice). A log-rank test was performed for comparison.

treated mice and, in addition, two mice out of six were cured by the Ad5PTD(D24) treatment (Fig. 6d). The better results for Ad5PTD(D24) compared to Ad5(mock) is most likely a combination of the PTD modification, D24 deletion of E1A, and the fact that Ad5PTD(D24) replicates, whereas Ad5(mock) does not.

DISCUSSION

Adenoviruses are widely used for gene transduction and oncolytic therapy. In order to selectively target certain cell types, many groups, including our own, have modified the viral capsid or fiber protein (8, 22, 28, 44). Most studies report modifications of either the HI loop or the C terminus of the adenovirus fiber. However, tumor selectivity can also be achieved by promoter-controlled E1A expression in tumor tissues or micro RNA target sequences to selectively degrade E1A expression in off-target tissues (7, 26, 27). The main aim of the present study was to increase viral transduction efficiency and to overcome the fiber-masking problem caused by excessive fiber proteins release from infected cells that blocks CAR on noninfected neighboring cells and prevents progeny virus entry (31). To achieve this, we decided to keep the targeting agent away from the fiber and to put it on the virus capsid. Although modification of the hexon HVR has been difficult to achieve (50), several groups have verified that the HVR5 site is tolerant for foreign peptide insertion (37, 45, 46, 50). Moreover, given the fact that there are 240 hexon trimers expressed on the adenoviral surface versus only 12 fiber trimer molecules and that hexon modification would not affect the native fiber binding, we decided to modify the hexon HVR5 site.

Our targeting peptide of choice is the protein transduction domain of the Tat protein from HIV-1 (Tat-PTD). Kurachi et al. have previously introduced Tat-PTD in the adenovirus fiber knob (23), and Eto et al. reported a method to modify adenovirus with Tat-PTD by chemical conjugation to lysine residues on exposed viral proteins (15). However, the chemical conjugation procedure is relatively complex, and the exact ratio of conjugated Tat-PTD peptide per viral particle could not be determined (15, 51). In our case, the Tat-PTD sequence was flanked by a short α-helix spacer and genetically inserted into the hexon HVR5 region. We hypothesized that the short α-helix spacer would expose the Tat-PTD motif, thereby increasing the virus-cell interactions, thus improving the transduction efficiency. The predicted model of the modified trimerized hexon (Fig. 1b) was obtained by superimposition of the Tet-PTD and linkers on the hexon trimer previously modeled by others. It shows that the Tat-PTD sequence in HVR5 is exposed on the top surface of the hexon, the portion of the protein facing the surrounding.

The transduction efficiency of Ad5PTD(GFP) was dramatically increased for CAR-negative cell lines compared to the unmodified virus Ad5(GFP). Interestingly, up to 90% of the SK-N-SH cells, which are nonpermissive for native adenovirus transduction, could be transduced by the Tat-PTD-modified Ad5PTD(GFP). In all other tested cell lines, the modified vector shows the same or better transduction efficiency than

the nonmodified Ad5(GFP) vector. The mechanism of cellular uptake and cell penetration of CPPs has been studied for decades and still remains divergent. Different models have been proposed to describe the mechanism. In general, these models can be categorized as energy-dependent endocytosis and direct translocation via the lipid bilayer (34). Another suggestion is that CPPs only play a role in "adherence" or "docking" to the cell surface while endocytosis mediates the actual cellular uptake (25). The secondary structure was also found to be important for different classes of CPPs (11). In our case, the exact transduction mechanism of the Tat-PTD modified viruses is unclear. We are able to transduce CAR-negative cells with the Tat-PTD-modified viruses and the transduction can only be partly blocked by soluble fiber molecules, which strongly indicates that a CAR-independent pathway is utilized for cellular uptake.

Recent data have demonstrated that the overproduced fiber molecules during the first round of viral infection are released prior to cell lysis and mask the receptor on adjacent uninfected cells and therefore inhibit the following rounds of infection (31). This phenomenon limits the usage of replicating oncolytic adenoviruses as anticancer agents. In contrast to chemically conjugated Tat-PTD-modified virus (15) or HI-loop/C-terminus Tat-PTD-modified virus (23), which would only enhance the first round of infection, we show that our Tat-PTD-modified virus, which utilizes a CAR-independent cellular transduction pathway, can overcome this problem. The plaque formation assay confirmed that Ad5PTD(wt) spreads faster than Ad5(wt) in a two-dimensional model, which suggests that the Tat-PTD-modified virus should spread faster also in three-dimentional structural tumors.

Hexon proteins were reported to play a major role in liver toxicity after intravenous administration of adenovirus (47). Liver infection, at least in mice, is mediated by binding of FX (Gla domain) to the HVR of the Ad5 hexon surface. The uptake of FX-Ad5 complexes in hepatocytes is mediated through a heparin-binding exosite in the FX serine protease domain. It has also been demonstrated that a single mutation on HVR5 or HVR7 could significantly reduce or totally abolish the FX binding ability (1). We evaluated the FX de-targeting ability of our HVR5 modified virus. Consistent with other reports, we found that the substitution of HVR5 by the Tat-PTD motif significantly reduces the FX-mediated virus cellular binding activity in two independent assays. In addition, the modification of the hexon removes antigenic epitopes on the virus particle surface, which leads to partial protection from preexisting neutralizing anti-Ad5 antibodies. Surprisingly, the protection from NAbs was not as efficient as was reported for the Tat-PTD chemically conjugated viruses (15) and the other hexon-modified viruses (32, 36). This is probably because the relatively small-sized modification cannot remove all natural Ad5 viral capsid epitopes.

We also examined the *in vivo* therapeutic effects of the Tat-PTD-modified oncolytic viruses on human neuroblastoma and neuroendocrine tumors. To our knowledge, this is the first study using adenoviruses modified with cell-penetrating peptides as oncolytic agents for cancer therapy. The human neuroblastoma cell line SK-N-SH was chosen for establishing xenografts since it is not transducible by native Ad5. We found that a therapeutic effect on SCID/beige mice with SK-N-SH xenografts can only be achieved by treatment with Tat-PTD-modified viruses, indicating that viral entry is crucial in order to achieve an oncolytic therapeutic effect. Since Ad5PTD(wt) is not tumor selective, we also produced and evaluated the Ad5PTD(D24) virus, along with Ad5(wt) and Ad5PTD(wt). We found that Ad5PTD(D24) is as efficient as Ad5PTD(wt), but not better (Fig. 6a and b). Therefore, only Ad5PTD(D24) was selected for treatment of neuroendocrine CDNT2.5 tumors on NMRI-nude mice. Geoerger et al. reported on an adenovirus AdΔ24-425S11 expressing a bispecific scFv which targets both the adenoviral fiber knob and the epidermal growth factor receptor, to generate higher transduction level on CAR-low neuroblastoma cells (21). However, the infectivity enhancement of that virus still relies on uptake via CAR at the first round of viral infection in order to produce the 425S11-targeting adapter. In contrast, the infectivity of our Tat-PTD-modified viruses is guaranteed also on CAR-low cells at the first viral infection step and will be carried on to viral progeny. Parikh et al. claimed that treatment of neuroblastoma by wild-type Ad5 was not as efficient as by oncolytic herpes simplex virus due to the lack of Ad5 transduction (29). We show in the present study that by enhancing Ad5 transduction, a therapeutic effect could be achieved for neuroblastoma.

It has been reported that the therapeutic effect achieved by treatment with oncolytic virus is partially dependent on the host immune response raised by viral infection (5, 41, 52). We evaluated the therapeutic effect on both nude and SCID/beige mouse models. Nude mice, lacking T cells but with functional B and NK cells, reflect the therapeutic effect from both viral oncolysis and a partially functioning host immune system. SCID/beige mice, deficient for T, B, and NK cells, are severely immunocompromised; thus, any therapeutic effect observed is solely dependent on viral oncolytic activity. Nude mice harboring CNDT2.5 xenografts treated with Ad5(mock) showed delayed tumor growth, indicating that a virally induced host immune response was involved. SCID/beige mice have also reported to have dysfunctional platelets and therefore prolonged bleeding time after needle puncture (18). All of the SCID/beige mice harboring tumor xenografts got wounds in the tumor area during tumor growth; therefore, the experiment had to be terminated immediately after the last mouse in the Ad5(wt) treatment group was sacrificed.

The changed tropism caused by genetic introduction of Tat-PTD in the Ad5 hexon raises potential safety concerns since the virulence and pathogenicity/transmission in the natural host as well as the host range may have changed. It is therefore important to combine the transductional alteration caused by Tat-PTD with a transcriptional modification in order to restrict virus activity in normal cells. In the present study we chose to combine it with the D24 deletion of E1A. An alternative approach would be to control E1A gene expression with a tissue- or tumor-specific promoter. In either case, the safety and virulence of Tat-PTD-modified Ad5 will have to be further examined and monitored before a clinical trial can be proposed. It should, however, be noted that Ad5 NAbs are also quite efficient in neutralizing Tat-PTD-modified Ad5. Ad5PTD(wt) shows significantly better shielding against Ad5 NAbs only under certain dilutions of sera (1:1,250 to 1:625). This means that under physiological conditions, Ad5 NAbs in the bloodstream will neutralize Tat-PTD-modified Ad5. Nev-

ertheless, it is very important to follow strict guidelines when working with Tat-PTD-modified replicating viruses.

In conclusion, we have developed Tat-PTD-modified oncolytic Ad5-based viruses with elevated infectivity. The viruses circumvent problems caused by excessive production and secretion of virus fiber protein in the first round of infection, fibers that could block receptors on neighboring noninfected cells and slow down subsequent replication rounds. They are particularly promising for the treatment of tumors with low CAR expression, as demonstrated here for experimental neuroblastoma and neuroendocrine tumors.

ACKNOWLEDGMENTS

We are grateful to Richard Stanton (Cardiff University, Cardiff, United Kingdom), Don Court (National Cancer Institute, Frederick, MD), Bhupender Singh and Linda Sandin (Uppsala University, Uppsala, Sweden), Ann-Charlotte Hellström (Alligator Bioscience AB, Lund, Sweden), and Hanna Björkelund and Karl Andersson (Uppsala University, Uppsala, Sweden, and Ridgeview Instruments AB, Uppsala, Sweden) for technical advice and assistance.

D.Y., N.M., and M.E. conceived and designed the experiments. D.Y., C.J., J.L., and B.N. performed the experiments and analyzed the data. D.Y., F.E., and M.E. wrote the paper. All authors read and approved the final version of the manuscript.

This study was supported by the Swedish Children Cancer Foundation (PROJ08/006 and PROJ10/027), the Swedish Cancer Society (contracts 10-0105 and 10-0552), the Gunnar Nilsson Cancer Foundation (grant 65/09), and the Swedish Research Council (grant K2008-68X-15270-04-3).

REFERENCES

1. **Alba, R., et al.** 2009. Identification of coagulation factor (F)X binding sites on the adenovirus serotype 5 hexon: effect of mutagenesis on FX interactions and gene transfer. Blood **114:**965–971.
2. **Bauerschmitz, G. J., et al.** 2004. Evaluation of a selectively oncolytic adenovirus for local and systemic treatment of cervical cancer. Int. J. Cancer **111:**303–309.
3. **Bjorke, H., and K. Andersson.** 2006. Automated, high-resolution cellular retention and uptake studies in vitro. Appl. Radiat. Isot. **64:**901–905.
4. **Boulanger, P. A., and F. Puvion.** 1973. Large-scale preparation of soluble adenovirus hexon, penton and fiber antigens in highly purified form. Eur. J. Biochem. **39:**37–42.
5. **Bridle, B. W., et al.** 2010. Potentiating cancer immunotherapy using an oncolytic virus. Mol. Ther. **18:**1430–1439.
6. **Carlsson, B., W. S. Cheng, T. H. Totterman, and M. Essand.** 2003. Ex vivo stimulation of cytomegalovirus (CMV)-specific T cells using CMV pp65-modified dendritic cells as stimulators. Br. J. Haematol. **121:**428–438.
7. **Cheng, W. S., et al.** 2004. A novel TARP-promoter-based adenovirus against hormone-dependent and hormone-refractory prostate cancer. Mol. Ther. **10:**355–364.
8. **Corjon, S., et al.** 2008. Targeting of adenovirus vectors to the LRP receptor family with the high-affinity ligand RAP via combined genetic and chemical modification of the pIX capsomere. Mol. Ther. **16:**1813–1824.
9. **Danielsson, A., H. Dzojic, B. Nilsson, and M. Essand.** 2008. Increased therapeutic efficacy of the prostate-specific oncolytic adenovirus Ad[I/PPT-E1A] by reduction of the insulator size and introduction of the full-length E3 region. Cancer Gene Ther. **15:**203–213.
10. **Danielsson, A., et al.** 2010. An ex vivo loop system models the toxicity and efficacy of PEGylated and unmodified adenovirus serotype 5 in whole human blood. Gene Ther. **17:**752–762.
11. **Eiriksdottir, E., K. Konate, U. Langel, G. Divita, and S. Deshayes.** 2010. Secondary structure of cell-penetrating peptides controls membrane interaction and insertion. Biochim. Biophys. Acta **1798:**1119–1128.
12. **El-Andaloussi, S., T. Holm, and U. Langel.** 2005. Cell-penetrating peptides: mechanisms and applications. Curr. Pharm. Des. **11:**3597–3611.
13. **Ellis, L. M., S. Samuel, and E. Sceusi.** Varying opinions on the authenticity of a human midgut carcinoid cell line. Clin. Cancer Res. **16:**5365–5366. (Letter.)
14. **Essand, M., J. Leja, V. Giandomenico, and K. E. Oberg.** 2011. Oncolytic viruses for the treatment of neuroendocrine tumors. Horm. Metab. Res. doi:10.1055/s-0031-1277225.
15. **Eto, Y., et al.** 2009. Transduction of adenovirus vectors modified with cell-penetrating peptides. Peptides **30:**1548–1552.
16. **Fallaux, F. J., et al.** 1996. Characterization of 911: a new helper cell line for the titration and propagation of early region 1-deleted adenoviral vectors. Hum. Gene Ther. **7:**215–222.
17. **Franqueville, L., et al.** 2008. Protein crystals in Adenovirus type 5-infected cells: requirements for intranuclear crystallogenesis, structural and functional analysis. PLoS One **3:**e2894.
18. **Froidevaux, S., and F. Loor.** 1991. A quick procedure for identifying doubly homozygous immunodeficient scid beige mice. J. Immunol. Methods **137:** 275–279.
19. **Fueyo, J., et al.** 2000. A mutant oncolytic adenovirus targeting the Rb pathway produces anti-glioma effect in vivo. Oncogene **19:**2–12.
20. **Fukazawa, T., et al.** 2010. Adenovirus-mediated cancer gene therapy and virotherapy. Int. J. Mol. Med. **25:**3–10.
21. **Geoerger, B., et al.** 2005. Expression of p53, or targeting toward EGFR, enhances the oncolytic potency of conditionally replicative adenovirus against neuroblastoma. J. Gene Med. **7:**584–594.
22. **Kreppel, F., J. Gackowski, E. Schmidt, and S. Kochanek.** 2005. Combined genetic and chemical capsid modifications enable flexible and efficient de- and retargeting of adenovirus vectors. Mol. Ther. **12:**107–117.
23. **Kurachi, S., et al.** 2007. Fiber-modified adenovirus vectors containing the TAT peptide derived from HIV-1 in the fiber knob have efficient gene transfer activity. Gene Ther. **14:**1160–1165.
24. **Lambert, C., N. Leonard, X. De Bolle, and E. Depiereux.** 2002. ESyPred3D: prediction of proteins 3D structures. Bioinformatics **18:**1250–1256.
25. **Leifert, J. A., S. Harkins, and J. L. Whitton.** 2002. Full-length proteins attached to the HIV tat protein transduction domain are neither transduced between cells, nor exhibit enhanced immunogenicity. Gene Ther. **9:**1422–1428.
26. **Leja, J., et al.** 2007. A novel chromogranin-A promoter-driven oncolytic adenovirus for midgut carcinoid therapy. Clin. Cancer Res. **13:**2455–2462.
27. **Leja, J., et al.** 2010. Double-detargeted oncolytic adenovirus shows replication arrest in liver cells and retains neuroendocrine cell killing ability. PLoS One **5:**e8916.
28. **Leja, J., et al.** 2011. Oncolytic adenovirus modified with somatostatin motifs for selective infection of neuroendocrine tumor cells. Gene Ther. doi: 10.1038/gt.2011.54.
29. **Parikh, N. S., et al.** 2005. Oncolytic herpes simplex virus mutants are more efficacious than wild-type adenovirus type 5 for the treatment of high-risk neuroblastomas in preclinical models. Pediatr. Blood Cancer **44:**469–478.
30. **Pesonen, S., et al.** 2010. Prolonged systemic circulation of chimeric oncolytic adenovirus Ad5/3-Cox2L-D24 in patients with metastatic and refractory solid tumors. Gene Ther. **17:**892–904.
31. **Rebetz, J., et al.** 2009. Fiber mediated receptor masking in non-infected bystander cells restricts adenovirus cell killing effect but promotes adenovirus host co-existence. PLoS One **4:**e8484.
32. **Roberts, D. M., et al.** 2006. Hexon-chimaeric adenovirus serotype 5 vectors circumvent preexisting anti-vector immunity. Nature **441:**239–243.
33. **Rux, J. J., P. R. Kuser, and R. M. Burnett.** 2003. Structural and phylogenetic analysis of adenovirus hexons by use of high-resolution x-ray crystallographic, molecular modeling, and sequence-based methods. J. Virol. **77:** 9553–9566.
34. **Sawant, R., and V. Torchilin.** 2010. Intracellular transduction using cell-penetrating peptides. Mol. Biosyst. **6:**628–640.
35. **Schaeffer, C., and M. A. Warso.** 2009. A phase I trial of p28 (cell penetrating peptide) in the treatment of refractory solid tumors. http://clinicaltrials.gov/ct2/show/ NCT00914914.
36. **Seregin, S. S., and A. Amalfitano.** 2009. Overcoming preexisting adenovirus immunity by genetic engineering of adenovirus-based vectors. Expert Opin. Biol. Ther. **9:**1521–1531.
37. **Shashkova, E. V., S. M. May, K. Doronin, and M. A. Barry.** 2009. Expanded anticancer therapeutic window of hexon-modified oncolytic adenovirus. Mol. Ther. **17:**2121–2130.
38. **Stanton, R. J., B. P. McSharry, M. Armstrong, P. Tomasec, and G. W. Wilkinson.** 2008. Re-engineering adenovirus vector systems to enable high-throughput analyses of gene function. Biotechniques **45:**659–. **62:**664–668.
39. **Terao, S., et al.** 2009. Improved gene transfer into renal carcinoma cells using adenovirus vector containing RGD motif. Anticancer Res. **29:**2997–3001.
40. **Thomas, M. A., D. L. Lichtenstein, P. Krajcsi, and W. S. Wold.** 2007. A real-time PCR method to rapidly titer adenovirus stocks. Methods Mol. Med. **130:**185–192.
41. **Thorne, S. H., et al.** 2010. Targeting localized immune suppression within the tumor through repeat cycles of immune cell-oncolytic virus combination therapy. Mol. Ther. **18:**1698–1705.
42. **Tollefson, A. E., M. Kuppuswamy, E. V. Shashkova, K. Doronin, and W. S. Wold.** 2007. Preparation and titration of CsCl-banded adenovirus stocks. Methods Mol. Med. **130:**223–235.
43. **Van Buren, G., 2nd, et al.** 2007. The development and characterization of a human midgut carcinoid cell line. Clin. Cancer Res. **13:**4704–4712.
44. **Vellinga, J., et al.** 2007. Efficient incorporation of a functional hyper-stable single-chain antibody fragment protein-IX fusion in the adenovirus capsid. Gene Ther. **14:**664–670.
45. **Vigant, F., et al.** 2008. Substitution of hexon hypervariable region 5 of

adenovirus serotype 5 abrogates blood factor binding and limits gene transfer to liver. Mol. Ther. **16:**1474–1480.

46. **Vigne, E., et al.** 1999. RGD inclusion in the hexon monomer provides adenovirus type 5-based vectors with a fiber knob-independent pathway for infection. J. Virol. **73:**5156–5161.
47. **Waddington, S. N., et al.** 2008. Adenovirus serotype 5 hexon mediates liver gene transfer. Cell **132:**397–409.
48. **Wang, H., et al.** 2011. Desmoglein 2 is a receptor for adenovirus serotypes 3, 7, 11, and 14. Nat. Med. **17:**96–104.
49. **Wang, H., et al.** 2007. Identification of CD46 binding sites within the adenovirus serotype 35 fiber knob. J. Virol. **81:**12785–12792.
50. **Wu, H., et al.** 2005. Identification of sites in adenovirus hexon for foreign peptide incorporation. J. Virol. **79:**3382–3390.
51. **Yoshioka, Y., et al.** 2008. Tat conjugation of adenovirus vector broadens tropism and enhances transduction efficiency. Life Sci. **83:**747–755.
52. **Zhang, Y. Q., Y. C. Tsai, A. Monie, T. C. Wu, and C. F. Hung.** 2010. Enhancing the therapeutic effect against ovarian cancer through a combination of viral oncolysis and antigen-specific immunotherapy. Mol. Ther. **18:**692–699.